Mechanism of amorphous $Ge_2Sb_2Te_5$ removal during chemical mechanical planarization in acidic H_2O_2 slurry*

He Ao-Dong(何敖东)[a)b)], Song Zhi-Tang(宋志棠)[a)], Liu Bo(刘 波)[a)†], Zhong Min(钟 旻)[a)], Wang Liang-Yong(王良咏)[a)], Lü Ye-Gang(吕业刚)[a)b)], and Feng Song-Lin(封松林)[a)]

[a)] *State Key Laboratory of Functional Materials for Informatics, Shanghai Institute of Micro-system and Information Technology, Chinese Academy of Sciences, Shanghai* 200050, *China*

[b)] *University of Chinese Academy of Sciences, Beijing* 100049, *China*

(Received 3 May 2012; revised manuscript received 27 June 2012)

In this paper, chemical mechanical planarization (CMP) of amorphous $Ge_2Sb_2Te_5$ (a-GST) in acidic H_2O_2 slurry is investigated. It was found that the removal rate of a-GST is strongly dependent on H_2O_2 concentration and gradually increases with the increase in H_2O_2 concentration, but the static etch rate first increases and then slowly decreases with the increase in H_2O_2 concentration. To understand the chemical reaction behavior of H_2O_2 on the a-GST surface, the potentiodynamic polarization curve, surface morphology and cross-section of a-GST immersed in acidic slurry are measured and the results reveal that a-GST exhibits a from active to passive behavior for from low to high concentration of H_2O_2. Finally, a possible removal mechanism of a-GST in different concentrations of H_2O_2 in the acidic slurry is described.

Keywords: H_2O_2, chemical mechanical planarization, $Ge_2Sb_2Te_5$

PACS: 85.40.–e, 81.65.–b, 52.77.Bn, 81.65.Cf **DOI:** 10.1088/1674-1056/22/1/018503

1. Introduction

Phase change memory (PCM), which is an emerging memory technology, has the potential to replace NOR flash and NAND flash if significant improvements in speed, endurance and density can be realized through the betterment of device scaling and materials.[1–3] PCM utilizes a special chalcogenide material that can repeatedly and rapidly switch between amorphous and crystalline phases with drastic change in electrical resistivity. Among chalcogenide materials, $Ge_2Sb_2Te_5$ (GST) alloy has been investigated intensively, because it seems to have the best combination of electrical, optical, and phase changing properties.[4–6] To decrease high reset current and increase the storage density, chemical mechanical planarization (CMP) has been applied to remove unwanted GST and planarize the GST surface after GST fills the damascene via.[7–10]

Recently, CMP of GST has been investigated in acidic and alkaline conditions. For the akaline condition, Cho *et al.*[11] investigated CMP of polycrystalline GST (p-GST) and found that the addition of H_2O_2 could increase the removal rate of p-GST. They concluded that removal of p-GST followed a corrosion mechanism through direct touching between p-GST film and abrasives at low concentration of H_2O_2 (below 0.2 wt%), but followed a cyclic polishing mechanism at high concentration of H_2O_2 beyond 0.2 wt%, involving a passivation by an oxidized GST layer, mechanical polishing between the oxidized GST surface and abrasives, and repassivation according to potentiodynamic behavior and X-ray photoelectron spectroscopy (XPS) results. However, Cui *et al.*[12] investigated CMP of nitrogen-doped polycrystalline GST (N-GST) using H_2O_2 and found that no Ge, Sb, or Te of oxides was formed using XPS result below 0.3 wt%; and the removal mechanism followed the corrosion polishing mechanism because the intensity of corrosion increases with the increasing H_2O_2 concentration but no data was shown above 0.3 wt%. For the acidic condition, Zhong *et al.*[13] investigated CMP of amorphous GST (a-GST) with addition of 2.0 wt% H_2O_2. Their results show that GeO_2, Sb_2O_5, and TeO_2 were formed on the a-GST surface after a-GST was dipped in the slurry for 10 min, but no detailed discussion about the removal mechanism was given. Cui *et al.*[14] investigated CMP of N-GST using nitric acidic slurry with 1.0 wt% H_2O_2 and found the addition of H_2O_2 could suppress selective pits corrosion of N-GST, and removal of N-GST followed a cyclic polishing mechanism with 1.0 wt% H_2O_2. However, few studies were reported on other concentrations of H_2O_2 such as that below 1.0 wt% in the acidic slurry. For akaline slurry, there are different removal mechanisms at low and high concentrations of H_2O_2, respectively. It is possible that there are also different removal mechanisms at different concentrations of H_2O_2 for the acidic slurry. Therefore, the CMP process of GST, especially the removal mechanism, needs to be further investigated

*Project supported by the National Basic Research Program of China (Grant Nos. 2010CB934300, 2011CBA00607, and 2011CB9328004), the National Integrate Circuit Research Program of China (Grant No. 2009ZX02023-003), the National Natural Science Foundation of China (Grant Nos. 60906004, 60906003, 61006087, 61076121, 61176122, and 61106001), and the Science and Technology Council of Shanghai, China (Grant Nos. 11DZ2261000 and 11QA1407800), and the Chinese Academy of Sciences (Grant No. 20110490761).

†Corresponding author. E-mail: liubo@mail.sim.ac.cn

© 2013 Chinese Physical Society and IOP Publishing Ltd

in the acidic slurry. In this paper, we investigate the CMP characteristic of a-GST in acidic H_2O_2 slurry and discuss the removal mechanisms in different concentrations of H_2O_2.

2. Experimental setup

For the polishing process with CMP tester (CETR, CP-4), the polishing parameters were set as follows: the down force was 1 psi; the pad rotation speed was 100 rpm; the wafer rotation speed was 100 rpm; the feed rate of the slurry was 100 ml/min; the polishing pad was IC1010; and the 400 nm a-GST film was 2.5 cm×3.0 cm in size. The material removal rates (MRR) shown were the average of 2 polish runs of 2-min duration each. The slurry included 1% colloidal silica which has a mean particle size of about 60 nm, and different concentrations of H_2O_2 and DI-water. Diluted HNO_3 was used to adjust the pH value. For the static etch experiment, a-GST samples 3.0 cm×3.0 cm in size were cleaned thoroughly in acetone, ethanol, and DI-water. The samples were dried with compressed N_2 and weighted in a microbalance (accuracy, ±0.01 mg). The a-GST was then immersed in acidic slurry with different concentrations of H_2O_2 for certain times. The surface morphology and cross section of a-GST immersed in an acidic solution were obtained with a scanning electron microscope (SEM, Hitachi S-4700, Japan).

Potentiodynamic measurements were conducted by using a potentiostat (Autolab PASTAT302N, Metrohm). This cell allowed a 1.0 cm×1.0 cm exposure area of the working electrode (a-GST film), the counter electrode consisted of a built-in Pt-coated mesh, and the reference electrode was Ag/AgCl. All potentials were measured relative to an Ag/AgCl electrode. The polarization curves were obtained with a voltage scan rate of 5 mV/s. The pH value of the solution was kept at 2.5. The removal rate (RR) and static etch rate (SER) of a-GST were calculated by the weight loss method.

3. Results and discussion

Figure 1 shows the RR and SER of a-GST as a function of H_2O_2 concentration in the acidic slurry. The RR of a-GST was only 15.4 nm/min without an oxidizer. With addition of H_2O_2, the RR was slightly increased to 17.4 nm/min at 0.5 wt%, and linearly increased between 0.5 wt% and 2.0 wt%, finally reaching 54.3 nm/min at 3.0 wt%. It apparently exhibits a saturation trend. For the a-GST etch in the acidic slurry, the SER of a-GST showed a different trend. The static etch rate of a-GST linearly increases from 3.8 nm/min at 0.5 wt% to a maximum of 14.4 nm/min at 1.5 wt% and then starts to decrease up to the 3.0 wt% H_2O_2. Cheng *et al.*[15] showed that a-GST was chemically inert in a pure acidic condition, and it could only be etched by nitric acid. However, Wang *et al.*[16] reported that almost all the acidic solutions could etch GST film with the addition of 10.0 vol% H_2O_2. Therefore, H_2O_2 can modify the a-GST surface due to the strong chemical reaction between a-GST and H_2O_2. The modified surface can be easily removed with the help of abrasives, which contributes to the high RR of the a-GST film.

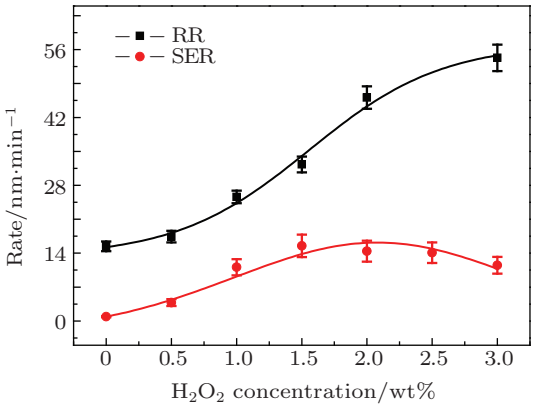


Fig. 1. (color online) Effect of H_2O_2 concentration on the removal rate (RR) and static etch rate (SER) of a-GST.

To systematically investigate the chemical reaction behavior between H_2O_2 and the a-GST surface, potentiodynamic polarization measurement, surface morphology and cross-section of a-GST dipped in the slurry were conducted to estimate the corrosion or oxidation characteristics on the a-GST film surface. Figure 2 presents the potentiodynamic polarization curves of a-GST dipped into the acidic slurries at room temperature. The corrosion potential (E_{corr}) and corrosion current density (I_{corr}) were calculated by extrapolating the cathodic and anodic branches of the polarization curves. It shows that the polarization curves are shifted towards a higher potential with the addition of H_2O_2. The E_{corr} as a function of H_2O_2 rapidly increases up to 1.0 wt% and almost saturates at 2.0 wt% H_2O_2 due to the high reduction capability of H_2O_2, as shown in Fig. 2(b). However, I_{corr} does not follow the same trend. The I_{corr} increases from 0.003 μA/cm^2 (without H_2O_2) to 0.242 μA/cm^2 (at 0.8 wt% H_2O_2), indicating that a-GST gradually dissolves in the acidic slurry because of the enhanced chemical reaction between a-GST and H_2O_2, which is responsible for the high RR. With a further increase in H_2O_2 concentration, I_{corr} sharply increases to 1.720 μA/cm^2 at 1.5 wt% H_2O_2, but rapidly decreases to 0.014 μA/cm^2 at 2.5 wt% H_2O_2, and then slowly decreases to 0.010 μA/cm^2 at 3.0 wt% H_2O_2, implying that a-GST exhibits a transition from active to passive behavior. At low concentration of H_2O_2, it indicates that the dissolution is active and a-GST dissolution is greatly enhanced due to high I_{corr}. However, I_{corr} decreases rapidly at high concentration of H_2O_2, which probably indicates that the a-GST surface is passivated with a chemical oxide layer rather than corroded. It is believed that the formation of a passive oxide layer increases the barrier to the transfer of ionic and electronic currents and thus leads to decreased I_{corr}.

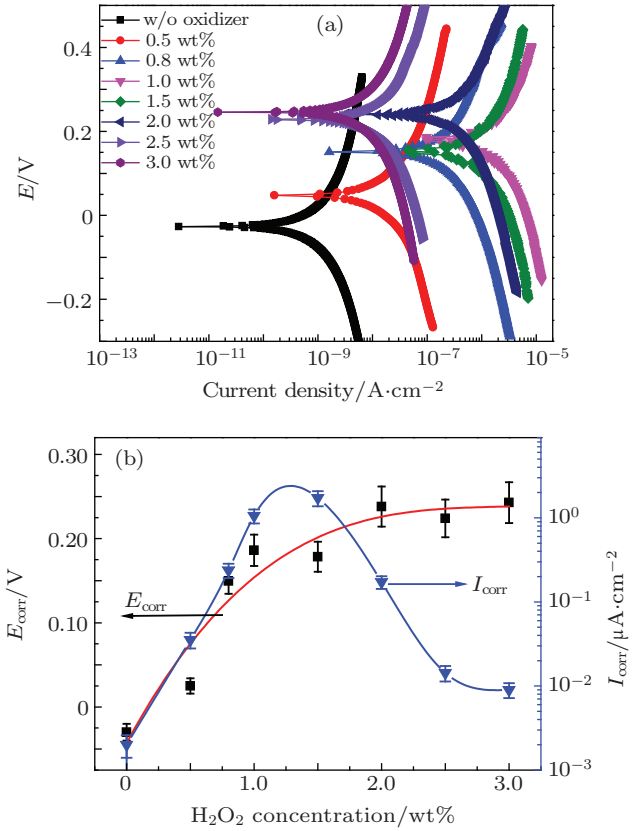


Fig. 2. (color online) Potentiodynamic polarization curves of a-GST dipped in the slurry. (a) Tafel curves of a-GST with different concentrations of H_2O_2, (b) corrosion potential (E_{corr}) and corrosion current (I_{corr}) with different concentrations of H_2O_2.

To confirm the formation of an a-GST surface oxide layer at different concentrations of H_2O_2, surface morphology and cross-section of a-GST dipped in the acidic slurry are shown with different H_2O_2 concentrations for 7 min at room temperature, as shown in Figs. 3 and 4. The surface and cross-section morphologies of a-GST are nearly the same without H_2O_2 in comparison with that of as-deposited a-GST. With 0.5 wt% H_2O_2, the a-GST surface is modified, little corrosion pits are found, and almost no oxide layer is observed, as shown in Figs. 3(c) and 4(c). With the increase in H_2O_2 concentration, it is found that a-GST is island-like, a porous oxide layer is produced on the a-GST surface (see Fig. 3(e)), especially at 1.5 wt% H_2O_2. Some serious corrosion pores are displayed on the cross-section (see Fig. 4(e)), which may result from dissolution of the resultant oxides. However, at above 2.5 wt% H_2O_2, the a-GST surface is covered by a dense thin oxide layer and only small corrosion pits are visible on the a-GST surface (see Figs. 3(g) and 3(h) and Figs. 4(g) and 4(h)), which indicates that the a-GST surface is passivated and the passivation layer prevents the ionic diffusion into solution. Thus, no pores are found on the a-GST inner, which matches well with that in Fig. 2. With regard to the component of the chemical oxide layer on the a-GST surface, Zhong *et al.*[13] reported that it was GeO_2, Sb_2O_5, and TeO_2 formed in the a-GST film surface in the acidic condition with 2.0 wt% H_2O_2. In our study, according to Pourbaix diagrams in a water system in the standard condition[14] for Ge, Sb, and Te, the corrosion potential of a-GST (less than 0.02 V) below 0.5 wt% H_2O_2 is located in the domain of GeO_2, Sb/Sb oxide boundary, and Te. In contrast, for above 0.8 wt% H_2O_2, the corrosion potential (0.18–0.24 V) is located in the domain of GeO_2, Sb_2O_5, and Te. It is obvious that the high concentration of H_2O_2 can result in the oxide formation of Ge and Sb. However, Te is relatively hard to be oxidized by H_2O_2 owing to the highest standard reduction potential among Ge, Sb, and Te elements.

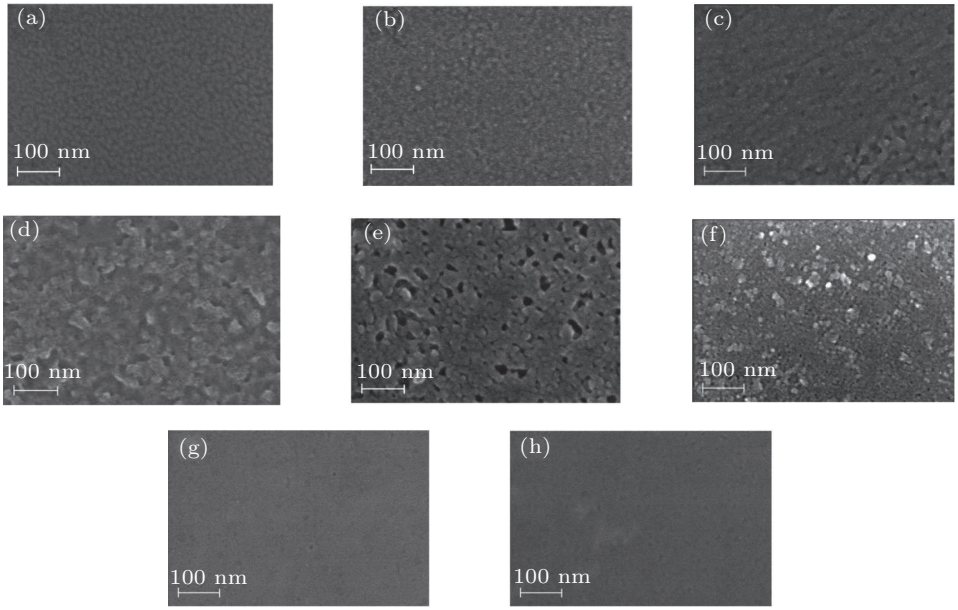


Fig. 3. Surface morphology of a-GST dipped in the acidic solution for 7 min in different H_2O_2 concentrations at room temperature: (a) no dipping, (b) 0%, (c) 0.5 wt%, (d) 1.0 wt%, (e) 1.5 wt%, (f) 2.0 wt%, (g) 2.5 wt%, (h) 3.0 wt%.

Generally, CMP of material is mainly dependent on the chemical and mechanical synergic interaction between the pad and wafer. The removal of GST involves the competition between the etching reaction which dissolves GST and the oxidation reaction to reform the corresponding oxides of Ge, Sb, and Te on the GST surface. In our study, when the H_2O_2 concentration is below 0.5 wt% in the acidic solution, almost no oxide layer is visible on the GST surface, the corrosion current density is very low, and the a-GST CMP mechanism is possibly dominated by mechanical abrasion. Above 1.0 wt% and below 2.0 wt% of H_2O_2, strong chemical reaction occurs between H_2O_2 and a-GST, partial a-GST dissolves in the slurry and there is oxidation of each element and subsequent dissolution of the resultant GeO_2 and Sb_2O_5. There is a competition between a-GST dissolution and oxide formation of each element. In this situation, a porous thin oxide layer is formed and serious corrosion pits are produced on the a-GST surface. The removal of a-GST seems to be controlled by a-GST and the corresponding partial oxide dissolution and mechanical removal of residual oxide. However, at high concentration of H_2O_2 (above 2.5 wt%), the oxidation rate of each element can be further enhanced due to acute chemical reaction, and the formation of the oxide layer is fast enough on the a-GST surface. Thus, the accumulative oxide keeps the a-GST surface passivated, and the removal of a-GST is controlled by mechanical removal of a-GST oxide with the help of abrasives and its subsequent dissolution.

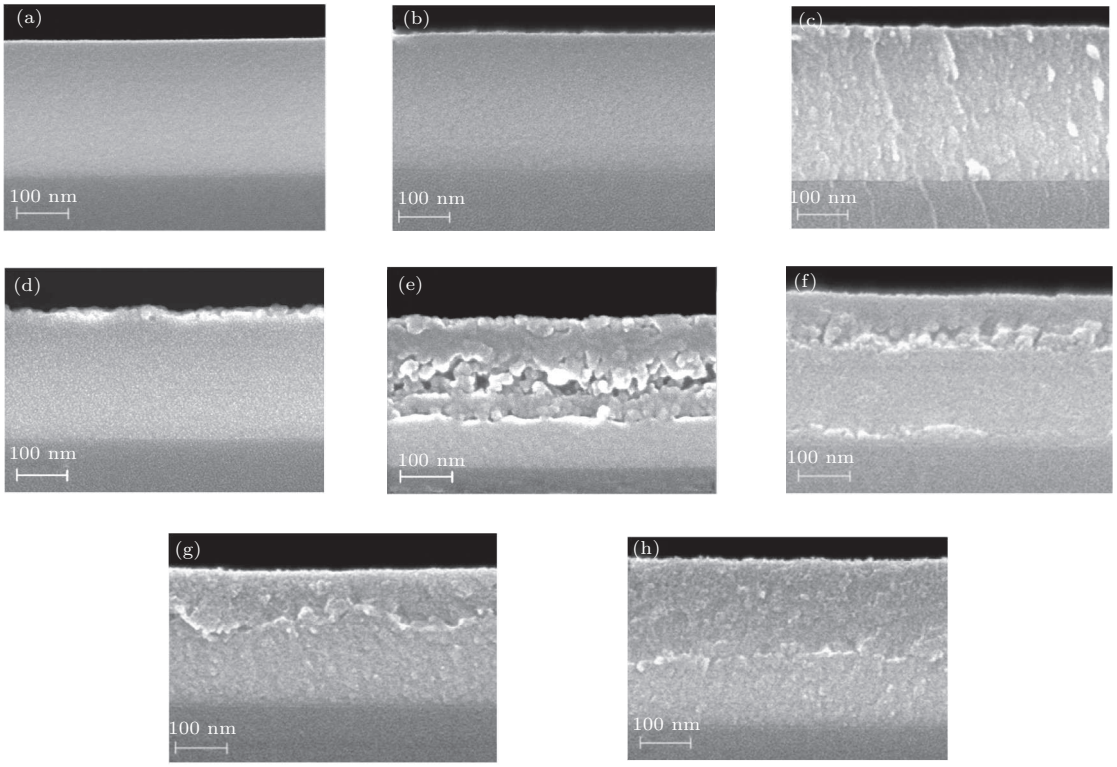


Fig. 4. Cross-section morphology of a-GST dipped in the acidic solution in different H_2O_2 concentrations for 7 min at room temperature: (a) no dipping, (b) 0%, (c) 0.5 wt%, (d) 1.0 wt%, (e) 1.5 wt%, (f) 2.0 wt%, (g) 2.5 wt%, (h) 3.0 wt%.

4. Conclusions

During the CMP of a-GST in the acidic H_2O_2 slurry, the removal rate of a-GST is strongly dependent on the H_2O_2 concentration and gradually increases with the increase in H_2O_2 concentration. Potentiodynamic polarization measurement, surface and cross-section morphology of a-GST immersed in acidic slurry with different H_2O_2 concentrations show that a-GST exhibits a from active to passive transition behavior for from low to high concentration of H_2O_2. Based on these results, a possible polishing mechanism of a-GST in acidic H_2O_2 slurry is presented. When the H_2O_2 concentration is low, e.g., below 0.5 wt%, the removal of a-GST during CMP is controlled by mechanical abrasion because the a-GST is chemically inert in a pure acidic condition. When the H_2O_2 concentration is medium, chemical reaction between the pad and the wafer is enhanced and there is a competition between the a-GST dissolution and oxide formation of each element. The removal of a-GST seems to be controlled by a-GST and the corresponding partial oxide dissolution and mechanical removal of residual oxide. When the H_2O_2 concentration is high, e.g., above 2.5 wt%, the formation of a-GST oxide is fast enough, and the removal of a-GST is controlled by mechanical removal

of a-GST oxide and its subsequent dissolution.

References

[1] Wong H, Raoux S, Kim S B, Liang J, Reifenberg J P, Rajendran B, Asheghi M and Goodson K E 2010 *Proc. IEEE* **98** 2201

[2] Gokirmak A, Bakan G, Zhu Y, Lai C S, Lam C H and Silva H 2012 *Thin Solid Films* **520** 2976

[3] Zhang T, Song Z T, Liu B, Liu W L, Feng S L and Chen B 2007 *Chin. Phys.* **16** 2475

[4] Friedrich I, Weidenhof V, Njoroge W, Franz P and Wuttig M 2000 *J. Appl. Phys.* **87** 4130

[5] Carria E, Mio A M, Gibilisco S, Miritello M, Grimaldi M G and Rimini E 2011 *Electrochem. Solid-State. Lett.* **14** H124

[6] Liu B, Song Z T, Zhang T, Feng S L and Gan F X 2004 *Chin. Phys.* **13** 1167

[7] Zhang K L, Liu Q B, Song Z T, Feng S L and Chen B 2006 *Solid-State and Integrated Circuit Technology* **ICSICT** 821

[8] Yeung F, Ahn S J, Hwang Y N, Jeong C W, Song Y J, Lee S S, Lee S H, Ryoo K C, Park J H, Shin J M, Jeong W C, Kim Y T, Koh G H, Jeong G T, Jeong H S and Kim K 2005 *Jpn. J. Appl. Phys.* **44** 2691

[9] Liu Q B, Song Z T, Zhang K L, Wang L Y, Feng S L and Chen B 2006 *Chin. Phys. Lett.* **23** 2296

[10] Zhong M, Song Z T, Liu Bo, Feng S L and Chen B 2008 *Chin. Phys. Lett.* **25** 762

[11] Cho J Y, Cui H, Park J H, Yi S H, and Park J G 2010 *Electrochem. Solid-State. Lett.* **13** H155

[12] Cui H, Cho J Y, Hwang H S, Lim J H, Park J H, Park H S, Hong K and Park J G 2010 *J. Electrochem. Soc.* **157** H1036

[13] Zhong M, Song Z T, Liu B, Feng S L and Chen B J 2008 *J. Electrochem. Soc.* **155** H929

[14] Cui H, Cho J Y, Park J H, Park H S and Park J G 2011 *J. Electrochem. Soc.* **158** H666

[15] Cheng H Y, Jong C A, Lee C M and Chin T S 2005 *IEEE Trans. Magn.* **41** 1031

[16] Wang L Y, Liu B, Song Z T, Feng S L, Xiang Y H and Zhang F X 2010 *J. Electrochem. Soc.* **157** H470